Journal of Biomedical Optics

BiomedicalOptics.SPIEDigitalLibrary.org

Visualization of the ocular pulse in the anterior chamber of the mouse eye *in vivo* using phase-sensitive optical coherence tomography

Peng Li
Zhihua Ding
Yang Ni
Baishen Xu
Chen Zhao
Yi Shen
Chixin Du
Bo Jiang

SPIE.

Visualization of the ocular pulse in the anterior chamber of the mouse eye *in vivo* using phase-sensitive optical coherence tomography

Peng Li,[a,*] Zhihua Ding,[a] Yang Ni,[a] Baishen Xu,[b] Chen Zhao,[a] Yi Shen,[a] Chixin Du,[b] and Bo Jiang[b]
[a]Zhejiang University, State Key Lab of Modern Optical Instrumentation, Department of Optical Engineering, Hangzhou, Zhejiang 310027, China
[b]Zhejiang University, College of Medicine, First Affiliated Hospital, Department of Ophthalmology, Hangzhou, Zhejiang 310027, China

Abstract. We report on a phase-based method for accurately measuring the ocular pulse in the anterior chamber *in vivo*. Using phase-sensitive optical coherence tomography with optimized scanning protocols and equations for compensating bulk motion and environmental vibrations, a high sensitivity of 0.9 μm/s minimal velocity is demonstrated at a wide detection band of 0 to 380 Hz. The pulsatile relative motion between cornea and crystalline lens in rodents is visualized and quantified. The relative motion is most likely caused by respiration (1.6 Hz) and heartbeat (6.6 Hz). The velocity amplitude of the relative motion is 10.3 ± 2.4 μm/s. The displacement amplitudes at the respiratory and cardiac frequencies are 202.5 ± 64.9 and 179.9 ± 49.4 nm, respectively. The potential applications of the measurement technique can be found in the evaluation of intraocular pressure and the measurement of biomechanical properties of the ocular tissue, which are important in several ocular diseases. [DOI: 10.1117/1.JBO.19.9.090502]

Keywords: optical coherence tomography; medical and biological imaging; ophthalmic optics and devices; tissue characterization; ocular pulse.

Paper 140426LR received Jul. 3, 2014; revised manuscript received Aug. 14, 2014; accepted for publication Aug. 19, 2014; published online Sep. 9, 2014.

Due to the ocular hemodynamics in the elastic eyeball, particularly the vascular volume changes of the choroid, several ocular elements experience a pulsatile movement, i.e., ocular pulse (OP).[1,2] OP is highly correlated with the biomechanical properties of the eye and may also act as a surrogate for changes in choroidal blood flow. The ability to noninvasively monitor the OP *in vivo* may play an important role in a number of ocular diseases such as glaucoma, age-related macular degeneration, and diabetic retinopathy. Fourier-domain optical coherence tomography (FDOCT) is a promising noninvasive method for high-resolution and dynamic eye imaging. Making use of the high-axial resolution of the FDOCT, the axial displacements of cornea and retina and the fundus pulse were measured by tracking the tissue position in sequential structural images.[3–5] Generally, the precision of the intensity-based measurement is limited and is highly dependent on the accuracy of image segmentation. In order to suppress the segment-error-induced noise, the movement was processed using a bandpass filter at cardiac frequency.[4,5] However, such a bandpass filter at certain frequencies is not desirable for the measurement of the minute OP in the anterior chamber (termed as aOP and defined as the relative motion between cornea and crystalline lens). As we know, the anterior chamber is filled with aqueous humor, and the aOP would be closely correlated to the intraocular pressure (IOP). Accordingly, similar to the IOP, the aOP may also be affected by several factors of different frequencies such as heartbeat and respiration.[6] Therefore, it would be particularly attractive to capture the aOP at a high sensitivity and a wide frequency-band to retain the valuable information which would otherwise be lost.

In contrast, the phase shift ϕ during a time interval τ is inherently sensitive to the subwavelength displacement D of scattering particles in the phase-sensitive OCT (PhS-OCT),[7,8], according to the relation expressed by $\phi = 4\pi n/\lambda_0 \times D$, where n is the refractive index of the ocular tissue which is typically 1.36, and λ_0 is the center wavelength used in OCT. The detectable displacement range of this phase-based method is bounded by the system signal-to-noise ratio (SNR) (lower limit, $\sim\lambda_0/4\pi n\sqrt{\mathrm{SNR}}$) and the π ambiguity (upper limit, $\sim\lambda_0/4n$).[8] Depending on the choice of the time interval τ, different velocity ranges can be achieved. However, there are several factors that make it challenging to visualize and quantify the dynamic aOP by the phase-based method. First, due to involuntary head movements and microsaccades, the small relative cornea-lens motion is accompanied with a large and time-variant bulk motion. Accordingly, the time interval (determined by the B-frame rate in PhS-OCT) should be carefully selected to make the velocity range cover both the slow relative motion and the fast bulk motion. Second, since the phase shift is calculated between successive B-frames in PhS-OCT, the accumulated phase drift $\phi_{\mathrm{drift}}(x, i)$ caused by the random environmental vibrations is no longer negligible during such a long-time interval and requires reliable compensation. Here, we report for the first time the application of PhS-OCT to visualize the dynamic aOP in the rodent eye *in vivo*, along with optimized scanning protocols and equations for compensating bulk motion and random vibrations.

Mice (strain C57BL/6) of 10 to 12 weeks of age were used in this experiment. All mice were raised and treated in compliance with the Association for Research in Vision and Ophthalmology statement. Mice were anesthetized by intraperitoneal injection. A total of six eyes were scanned by PhS-OCT. The PhS-OCT system is based on a spectral-domain configuration, similar to the system in Ref. 7. A broadband superluminescent light source with a central wavelength of 850 nm and a spectral bandwidth of 100 nm was used to achieve an axial resolution of ~3.2 μm in air. A high-speed spectrometer is used to record the OCT spectrum, providing a 70-kHz line scan rate and a measured imaging range of ~6.19 mm in air at half Fourier space.

*Address all correspondence to: Peng Li, E-mail: peng_li@zju.edu.cn

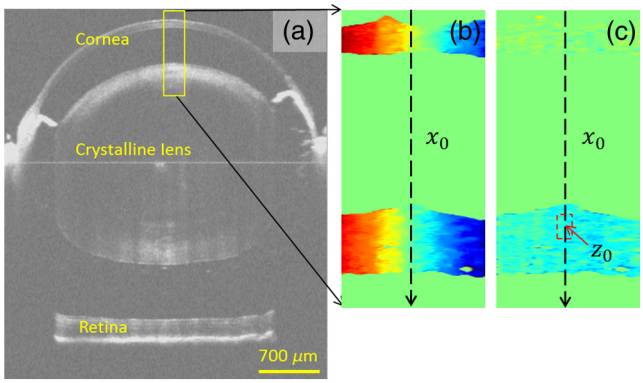

Fig. 1 (a) Wide-field structural cross-section in the horizontal meridian using a full-range complex method (refer to Ref. 9) to illustrate the architecture of the full mouse eye. Phase cross-section of the regional anterior chamber (as marked by the rectangle in a) before (b) and after (c) phase compensation.

Based on the structural image, the cornea and lens components are generally ~30 dB above the noise floor [refer to Fig. 2(a)], i.e., the system phase noise can be considered as 0.03 rad. By tracking the cornea/lens position in the M-mode structural image [refer to Fig. 2(a)], the maximal velocity of the bulk motion can reach ~107 μm/s, whereas the velocity of the relative motion is in the range of several micrometers per second [refer to Fig. 2(c)]. To capture both the bulk and the relative motions, a B-frame rate of 780 fps was used to provide a theoretical detectable velocity range of 1.2 to 122 μm/s at a wide detection band of 0 to 390 Hz (Nyquist theorem). Moreover, the slow scanning was stopped for repeated B-scanning in the horizontal meridians. In total, 3000 frames were collected covering a dynamic optical interval of ~3.85 s.

Figure 1(a) shows a wide-field OCT image of the full mouse eye using a full-range complex method, which has been detailed in Ref. 9 and is not elaborated here. In this study, the field of view is focused on the central part of anterior chamber [as marked by the rectangle in Fig. 1(a)] for dynamic imaging. As shown in Fig. 1(b), the raw phase cross-section $\phi_0(x,z,i)$ can be generated based on the equation

$$\phi_0(x,z,i) = \arg[r(x,z,i)r^*(x,z,i+1)], \tag{1}$$

where $r(x,z,i)$ is the complex OCT cross-sectional signal at the i'th acquisition of successive frames. The acquisition number i can be related to the time t by $t = i\tau$, and τ is the time interval between successive frames. $*$ denotes the complex conjugation of a complex signal. arg represents the operation of phase extraction. According to the depth information in the phase images $\phi_0(x,z,i)$, the raw cornea phase $\phi_{c0}(x,i)$ and the raw lens phase $\phi_{l0}(x,i)$ can be separated and, respectively, expressed as

$$\phi_{c0}(x,i) = \phi_B(x,i) + \phi_{\text{drift}}(x,i) \tag{2}$$

$$\phi_{l0}(x,i) = \Delta\phi_{lc}(x,i) + \phi_B(x,i) + \phi_{\text{drift}}(x,i), \tag{3}$$

where $\Delta\phi_{lc}(x,i)$ is the phase difference corresponding to the relative motion between the cornea and the lens. $\phi_B(x,i)$ and $\phi_{\text{drift}}(x,i)$ are the phase changes as a result of the bulk motion and the random vibrations, respectively. Therefore, as shown in Fig. 1(c), the relative phase difference $\Delta\phi_{lc}(x,i)$ can be extracted based on the following equation:

$$\Delta\phi_{cl}(x,i) = \arg\{r(x,z,i)r^*(x,z,i+1)\exp[-\phi_{c0}(x,i)]\}, \tag{4}$$

where the raw cornea phase $\phi_{c0}(x,i)$ is reliably determined by a histogram-based phase selecting process.[7,10]

In order to visualize the time-variant aOP, M-mode structural and phase images are generated along the center A-line of the B-frame (denoted as x_0) as shown in Figs. 2(a) and 2(b). The anterior and posterior corneal boundaries as well as the anterior lens boundary are segmented based on the derivative of the intensity signal in the z-direction. As indicated in Fig. 2(b), the residual phase of the cornea component is around zero (green color), and the lens component presents a periodical variation versus time after compensation. Therefore, the compensated lens motion can be regarded as the relative cornea-lens motion, i.e., the aOP. To further quantify the aOP, the relative cornea-lens velocity (ΔV_{cl}) is plotted versus time along the depth z_0 [around the center part of the anterior lens, marked by the red bold arrows in Fig. 2(b)], based on the following equation:

$$\Delta V_{cl}(i) = \lambda_0/4\pi n\tau \times \Delta\phi_{cl}(i), \tag{5}$$

as reported by the red curve in Fig. 2(c). The residual cornea velocity is also plotted with a root-mean-square level of 0.9 μm/s (i.e., minimal detectable velocity), as shown by the blue dashed line in Fig. 2(c). According to the power spectrum analysis, the relative velocity ΔV_{cl} is mainly composed of two frequency components at 1.6 and 6.6 Hz, respectively. The low-frequency component 1.6 Hz is most likely due to the mouse respiration, whereas the 6.6-Hz frequency component is induced by the heartbeat. The relative displacement (ΔD_{cl}) pulse is readily obtained by integrating the velocity ΔV_{cl} versus the time t, as shown in Fig. 3(a). The waveform of the pulsatile

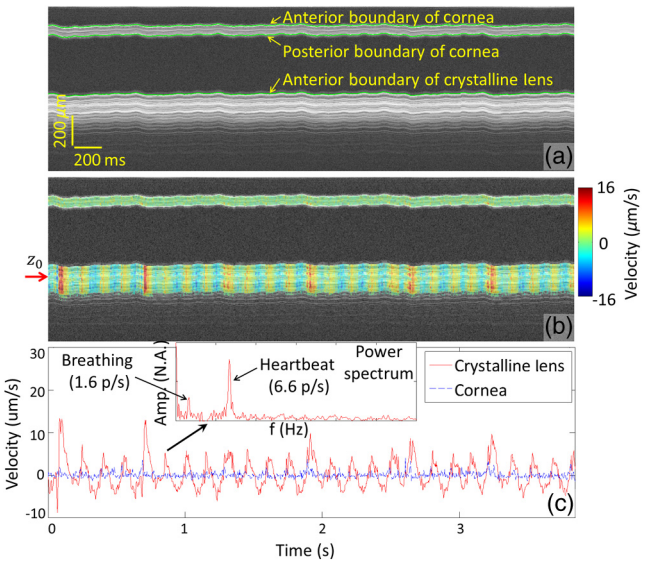

Fig. 2 Dynamic ocular pulse in the anterior chamber (aOP) image. (a) M-mode structural image generated along the center A-line of the B-frame. (b) M-mode structural image with phase encoded as hue. (c) The relative cornea-lens velocity (red line) and the residual cornea velocity (blue dashed line) versus time. The inset is the power spectrum of the relative velocity.

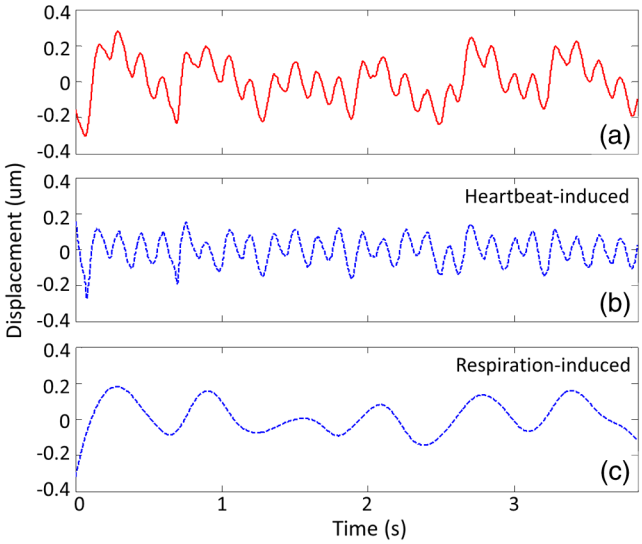

Fig. 3 Relative cornea-lens displacement. (a) Original displacement deduced from the velocity curve of Fig. 2(c) can be decomposed into two components: the heartbeat-induced (b) and the respiration-induced (c).

ΔD_{cl} is quite similar to the IOP variations due to the heartbeat and respiration, as reported in Ref. 6. According to the frequency analysis, the relative displacement is further decomposed into two components: the heartbeat-induced and the respiration-induced, as respectively shown in Figs. 3(b) and 3(c). According to the statistics generated from a total of six mouse eyes, the velocity amplitude is 10.3 ± 2.4 μm/s. The displacement amplitudes at the respiratory and cardiac frequencies are, respectively, 202.5 ± 64.9 and 179.9 ± 49.4 nm.

This preliminary study demonstrates the feasibility of using a phase-based method for aOP imaging/measurement *in vivo*. The method provides a high sensitivity of 0.9 μm/s minimal velocity at a wide detection band of 0 to 380 Hz. Further research could be performed to correlate the aOP to the fundus pulse, the choroidal blood flow, the IOP, and the biomechanical properties of the ocular tissue.

We acknowledge financial supports from the Chinese Natural Science Foundation (61335003, 61275196, and 61327007), Zhejiang Province Science and Technology Grant (2012C33031), Zhejiang Provincial Natural Science Foundation of China (LY14F050007), and the Fundamental Research Funds for the Central Universities (2014QNA5017).

References

1. D. M. Silver and R. A. Farrell, "Validity of pulsatile ocular blood flow measurements," *Surv. Ophthalmol.* **38**(Suppl), S72–S80 (1994).
2. J. C. Li et al., "The dynamic response of intraocular pressure and ocular pulse amplitude to acute hemodynamic changes in normal and glaucomatous eyes," *Invest. Ophthalmol. Visual Sci.* **54**(10), 6960–6967 (2013).
3. R. de Kinkelder et al., "Heartbeat-induced axial motion artifacts in optical coherence tomography measurements of the retina," *Invest. Ophthalmol. Visual Sci.* **52**(6), 3908–3913 (2011).
4. K. Singh et al., "Development of a novel instrument to measure the pulsatile movement of ocular tissues," *Exp. Eye Res.* **91**(1), 63–68 (2010).
5. K. Singh et al., "Measurement of ocular fundus pulsation in healthy subjects using a novel Fourier-domain optical coherence tomography," *Invest. Ophthalmol. Visual Sci.* **52**(12), 8927–8932 (2011).
6. R. L. Cooper et al., "Continual monitoring of intraocular pressure: effect of central venous pressure, respiration, and eye movements on continual recordings of intraocular pressure in the rabbit, dog, and man," *Br. J. Ophthalmol.* **63**(12), 799–804 (1979).
7. P. Li et al., "Pulsatile motion of the trabecular meshwork in healthy human subjects quantified by phase-sensitive optical coherence tomography," *Biomed. Opt. Express* **4**(10), 2051–2065 (2013).
8. K. E. O'Hara et al., "Measuring pulse-induced natural relative motions within human ocular tissue in vivo using phase-sensitive optical coherence tomography," *J. Biomed. Opt.* **18**(12), 121506 (2013).
9. P. Li et al., "Extended imaging depth to 12 mm for 1050-nm spectral domain optical coherence tomography for imaging the whole anterior segment of the human eye at 120-kHz A-scan rate," *J. Biomed. Opt.* **18**(1), 016012 (2013).
10. V. X. D. Yang et al., "Improved phase-resolved optical Doppler tomography using the Kasai velocity estimator and histogram segmentation," *Opt. Commun.* **208**(4–6), 209–214 (2002).